

ANALYSIS OF CONTINUOUS REVERSE OSMOSIS SYSTEMS FOR DESALINATION*

WILLIAM N. GILL†, CHI TIEN‡ and DALE W. ZEH‡

(Received 9 April 1965 and in revised form 24 November 1965)

Abstract—Analyses of continuous constant pressure reverse osmosis two-dimensional flow systems are given such that system performance is predicted explicitly in terms of operating variables. Such problems require the solution of a nonlinear diffusion equation with nonlinear boundary conditions. A series solution, which accounts for nonlinearities in both the diffusion equation and its boundary conditions, is developed.

Boundary-layer flows with pressure gradient are treated as wedge type flows, and the analyses given can be applied to both fully developed and entrance region flows. Generalized numerical results are given for a wide range of practical interest. Some specific data are also reported for typical systems similar to those which may be used in practice.

NOMENCLATURE

A , membrane constant defined by equation (4);
 B_2 , $= \pi_0/\Delta P$;
 D , diffusion coefficient;
 E , fraction of feed converted to fresh water divided by the fraction that would be converted if the wall velocity were $v_w(0)$ along the entire conduit;
 n_s , mass flux of salt defined by equation (5);
 N_{Pe} , Péclet number, $\frac{4U_b R}{D}$;
 N_{Re} , Reynolds number, $\frac{4U_b R}{\nu}$;
 $N_{Re_x} = \frac{U_\infty x p}{\mu}$;
 N_{Sc} , Schmidt number, ν/D ;
 ΔP , total pressure drop across membrane;
 Q , volume of water produced per unit time per unit width of membrane;
 R , half channel width;
 u , axial velocity;
 u_δ , core velocity in entrance region of

flat duct;
 U_b , bulk velocity of brine in parallel plate channel at $x = 0$;
 v , transverse velocity;
 $v_w(0)$, transverse velocity at wall at entrance to system;
 w_s , mass fraction of salt in brine;
 x , axial distance coordinate;
 $x_1 = 16 \frac{x/4 R}{4 R U_b/\nu}$;
 y , transverse distance coordinate.

Greek symbols

ρ , density;
 μ , viscosity;
 π , osmotic pressure of a saline solution;
 π_0 , osmotic pressure at $x = 0$;
 θ , dimensionless mass fraction, $w_s/w_s(0, y)$;
 τ_w , shear stress at membrane wall;
 ν , kinematic viscosity;
 η , dimensionless coordinate, $y [(A \Delta P)/D]$;
 σ , $= (9 \lambda)^\dagger$;
 β , $= \eta \sigma^{-1}$;
 α , $= D/(v_w(0) R)$;
 λ , $= \frac{(A \Delta P)^3 \mu}{D^2} \int_0^x \frac{dx}{\tau_w(x)}$;

* Work supported by Office of Saline Water, U.S. Department of Interior.

† Clarkson College of Technology, Potsdam, New York.

‡ Syracuse University, New York.

δ , momentum boundary-layer thickness.

Subscripts

- b , bulk value;
- w , value at membrane surface;
- ∞ , free stream quantity.

ANALYSIS

CURRENTLY, one of the more promising processes for purifying saline water solutions is the reverse osmosis or ultra-filtration process. In principle, reverse osmosis is very simple and its most attractive feature is that no obvious phase change is required in order to separate the salt and water. Separations in reverse osmosis systems involve the use of selective membranes which, in the ideal case, are permeable to water but not salt. Practical designs will no doubt employ continuous systems but the geometry of such systems may vary quite considerably. Therefore, it is desirable to develop mathematical solutions which are general enough to apply to various flow conditions and geometrical configurations.

For the case of fully developed flow between parallel plates with uniform surface flux of water, which leads to a linear boundary condition, Dresner *et al.* [1, 4] have shown that an asymptotic solution to the diffusion equation for small x is in fact valid for a substantial distance from the inlet of the system. Subsequently, this solution was generalized to account for variable water surface flux by a perturbation method [2]. In the present work asymptotic solutions, valid for very large Schmidt number systems, are determined for two dimensional flows by a series expansion method.

The water flux through the membrane is taken to be proportional to the total pressure drop across the membrane minus the osmotic pressure at the wall. Since the salt concentration at the wall increases in the axial direction, the effective osmotic pressure also increases. Consequently, the water flux and the transverse velocity at the wall decrease along the direction of main flow and, therefore, the diffusional problem considered here is nonlinear.

Since the Schmidt number for salt water is about 560, the diffusion boundary layer is much thinner than the momentum boundary layer and, therefore, the velocity components can be represented by expressions which are accurate only in the region near the wall. Exact asymptotic velocity components are used in both the diffusion equation and the boundary condition at the wall.

Figure 1 shows the coordinate system used. If the diffusion boundary layer is very thin, then

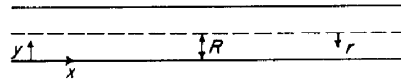


FIG. 1. Coordinate system.

one can neglect the effect of any transverse curvature of the conduit, and the continuity, momentum and diffusion equations can be written in terms of these coordinates for a constant fluid property system, as

$$\frac{\partial u}{\partial x} + \frac{\partial v}{\partial y} = 0 \tag{1}$$

$$u \frac{\partial u}{\partial x} + v \frac{\partial u}{\partial y} = -\frac{1}{\rho} \frac{\partial P}{\partial x} + \nu \frac{\partial^2 u}{\partial y^2} \tag{2}$$

$$u \frac{\partial w_s}{\partial x} + v \frac{\partial w_s}{\partial y} = D \frac{\partial^2 w_s}{\partial y^2} \tag{3}$$

Flow through the membrane is described by

$$-v_w = A [\Delta P - \pi_0 \theta(x, 0)] = A \Delta P [1 - B_2 \theta(x, 0)]. \tag{4}$$

The mass flux of salt in the y -direction is given by

$$n_s = w_s \rho v - \rho D \frac{\partial w_s}{\partial y} \tag{5}$$

but for an ideal membrane the flux of salt vanishes at the wall so that equation (5) yields

$$D \frac{\partial w_s(x, 0)}{\partial y} = v_w w_s(x, 0). \tag{6}$$

If one combines equations (4) and (6) the result is

$$-D \frac{\partial w_s(x, 0)}{\partial y} = A w_s(x, 0) [\Delta P - \pi_0 \theta(x, 0)]. \tag{7}$$

It was mentioned previously that the Schmidt number is large and, therefore, the velocity distribution near the wall is most important. In the region near the wall

$$u = [\tau_w(x)/\mu]y \quad (8)$$

and from equation (1)

$$v = v_w - \frac{1}{\mu} \frac{d\tau_w}{dx} \frac{y^2}{2}. \quad (9)$$

Let

$$\lambda = \frac{(A \Delta P)^3 \mu}{D^2} \int_0^x \frac{dx}{\tau_w(x)}, \quad \eta = \frac{yA \Delta P}{D}$$

and then by combining equations (3), (8) and (9) one gets

$$\eta \frac{\partial \theta}{\partial \lambda} = \left[1 - B_2 \theta(\lambda, 0) + \frac{\eta^2}{2\tau_w} \frac{d\tau_w}{d\lambda} \right] \frac{\partial \theta}{\partial \eta} + \frac{\partial^2 \theta}{\partial \eta^2} \quad (10)$$

with the boundary conditions

$$\theta(0, \eta) = 1 \quad (11)$$

$$\frac{\partial \theta}{\partial \eta}(\lambda, \infty) = 0 \quad (12)$$

$$-\frac{\partial \theta}{\partial \eta}(\lambda, 0) = \theta(\lambda, 0) [1 - B_2 \theta(\lambda, 0)] \quad (13)$$

Equation (10) is similar to, but considerably more general than, the differential equation for which Dresner obtained asymptotic solutions for the entrance region that are useful for considerable distances downstream. In particular, equations (10) to (13) are identical to Dresner's if $B_2 = 0$ and $d\tau_w/dx = 0$. However, since both equations (10) and (13) are nonlinear Dresner's approach, which utilizes the Laplace transform, cannot be employed here. Thus, a series expansion method will be developed which can be used to solve a somewhat broader class of problems than the reverse osmosis problem which is of direct interest here.

For simplicity we shall restrict attention to

wedge type flows and, if the effect of the very small v_w on τ_w is assumed to be negligible, such flows can be described by

$$U_\infty = Cx^n$$

$$\frac{u}{U_\infty} = \phi'(\xi)$$

$$\xi = y \sqrt{\left[\frac{1+n}{2} \frac{U_\infty}{\nu x} \right]}$$

$$\tau_w = C^{\frac{1}{2}} \phi''(0) x^{(3n-1)/2} \sqrt{\left[\frac{1+n}{2} \mu \rho \right]} \quad (14)$$

Clearly, when $n = \frac{1}{3}$, τ_w is constant. Aside from characterizing a particular wedge angle, constant wall shear corresponds to the important practical case of fully developed flow between parallel plates if the correct expression for τ_w is used. As mentioned previously, for $B_2 = 0$ this case was treated by Dresner [4] who neglected the effect of v_w on τ_w , so that

$$\tau_w = \frac{3 U_b \mu}{R}$$

This case is important because it is the one in which $d\tau_w/dx$ is a maximum for fully developed conduit flows since v_w does not decrease along the axial direction. Also, the problem is linear and the fully developed velocity field is known exactly [5] for $B_2 = 0$, so that one can easily obtain an exact solution of equation (3) in terms of orthogonal functions. This exact solution was used to test the assumption of neglecting $d\tau_w/dx$ in equation (10) and it was found to be a good assumption except at relatively large distances from the inlet where the exact solution begins to approach its asymptotic form and equation (8) is no longer valid. This is not too surprising because even with v_w/U_b as large as 5×10^{-5} , it can easily be shown that τ_w will be constant to within 5 per cent of $\tau_w(0)$ for 1000 radii downstream from the entrance and thus the term in equation (10) involving $d\tau_w/dx$ can be neglected for all values of B_2 when the velocity distribution is fully developed at the entrance to the membrane test section.

The effect of v_w on τ_w will be maximal for the case of uniform wall velocity, that is, $B_2 = 0$, and in this case it can be seen in Fig. 13.9 of reference [7] that, when $v_w/U_b < 10^{-4}$, the shear stress on a flat plate ($n = 0$) is negligibly affected throughout the laminar region. Thus, having shown that the shear stress in a conduit, with $n = \frac{1}{3}$, and on a flat plate, with $n = 0$, is negligibly affected by the interfacial velocities that occur in reverse osmosis systems, it is reasonable to assume that the shear stress for systems wherein $0 < n < \frac{1}{3}$ will be similarly unaffected.

Let

$$\sigma = (9\lambda)^{\frac{1}{3}}, \quad \beta = \eta\sigma^{-1}$$

and equation (10) is transformed to

$$3 \sigma \beta \frac{\partial \theta}{\partial \sigma} = \left\{ \sigma [1 - B_2 \theta(\sigma, 0)] + \left[3 + \frac{9}{2} \frac{3n - 1}{3(1 - n)} \right] \beta^2 \right\} \frac{\partial \theta}{\partial \beta} + \frac{\partial^2 \theta}{\partial \beta^2} \quad (15)$$

The boundary conditions, equations (11) to (13), become

$$\theta(0, \infty) = 1 \quad (16)$$

$$\frac{\partial \theta}{\partial \beta}(\sigma, \infty) = 0 \quad (17)$$

$$-\frac{\partial \theta}{\partial \beta}(\sigma, 0) = \sigma \theta(\sigma, 0) [1 - B_2 \theta(\sigma, 0)] \quad (18)$$

If

$$\theta = \sum_{k=0}^{\infty} \theta_k(\beta) \sigma^k$$

then $\theta_0 = 1$ and

$$\theta_1'' + \left[3 + \frac{9}{2} \left(\frac{3n - 1}{3(1 - n)} \right) \right] \beta^2 \theta_1' - 3 \beta \theta_1 = 0 \quad (19a)$$

$$\theta_2'' + \left[3 + \frac{9}{2} \left(\frac{3n - 1}{3(1 - n)} \right) \right] \beta^2 \theta_2' - 6 \beta \theta_2 = (B_2 - 1) \theta_1' \quad (19b)$$

$$\theta_i'' + \left[3 + \frac{9}{2} \left(\frac{3n - 1}{3(1 - n)} \right) \right] \beta^2 \theta_i' - 3 i \beta \theta_i = (B_2 - 1) \theta_{i-1}' + B_2 \sum_{j=1}^{i-2} \theta_j(0) \theta_{i-j-1}'$$

The boundary conditions become

$$\theta_k'(\infty) = 0 \quad (20)$$

$$-\theta_1'(0) = 1 - B_2 \quad (21a)$$

$$-\theta_2'(0) = (1 - 2 B_2) \theta_1(0) \quad (21b)$$

$$-\theta_i'(0) = (1 - 2 B_2) \theta_{i-1}(0)$$

$$- B_2 \sum_{j=1}^{i-2} \theta_j(0) \theta_{i-j-1}(0).$$

For $n = \frac{1}{3}$ the solution for θ_1 can be obtained in closed form, in terms of the incomplete gamma function $\Gamma(\frac{2}{3}, \beta^3)$, as

$$\frac{\theta_1}{1 - B_2} = \frac{\exp[-\beta^3]}{\Gamma(\frac{2}{3})} - \beta \left[1 - \frac{\Gamma(\frac{2}{3}, \beta^3)}{\Gamma(\frac{2}{3})} \right] \quad (22)$$

One can determine as many terms of the series expansion as desired, but since each successive solution depends on those preceding it, error accumulates and it would be difficult to obtain many more than the first ten terms with reasonable accuracy.

Since equations (19) with the boundary conditions in equations (20) and (21) are linear, a superposition method may be used to obtain solutions independent of B_2 . For example, we could let

$$\theta_1 = (1 - B_2) \phi_1$$

and obtain

$$\phi_1'' + \left[3 + \frac{3}{2} \left(\frac{3n - 1}{1 - n} \right) \right] \beta^2 \phi_1' - 3 \beta \phi_1 = 0$$

$$-\phi_1'(0) = 1$$

$$\phi_1'(\infty) = 0$$

Similarly, let

$$\theta_2 = (1 - B_2) [\phi_{21} + B_2 \phi_{22}]$$

Then ϕ_{21} and ϕ_{22} satisfy the following equations:

$$\phi_{21}'' + \left[3 + \frac{3}{2} \left(\frac{3n - 1}{1 - n} \right) \right] \beta^2 \phi_{21}' - 6 \beta \phi_{21} = -\phi_1'$$

$$-\phi_{21}'(0) = \phi_1(0)$$

$$\phi_{21}'(\infty) = 0$$

$$\begin{aligned} \phi''_{22} + \left[3 + \frac{3}{2} \left(\frac{3n-1}{1-n} \right) \right] \beta^2 \phi'_{22} - 6\beta \phi_{22} &= \phi'_1 \\ -\phi'_{22}(0) &= -2\phi_1(0) \\ \phi'_{22}(\infty) &= 0. \end{aligned}$$

The same procedure may be followed for all θ_i , the general form for each being

$$\theta_i = (1 - B_2) \sum_{j=1}^i B_2^{j-1} \phi_{ij} \quad (23)$$

Equations (19) to (21) were solved for various B_2 up to and including θ_9 , for $n = \frac{1}{3}$, and θ_5 for $n = 0$. The values of $\phi_{ij}(0)$, as defined by equation (23), are given up to $i, j = 5$. Also, to get an idea of the manner in which the form of v affects the solution the case of $v = 0$ in equation (15) [which amounts to neglecting the inhomogeneities in equations (19)] was also solved for the θ_k functions up to and including θ_5 . It is important to note that this analysis which employs the linear velocity of equation (8), is exact for $N_{Sc} = \infty$. For saline water solutions $N_{Sc} \approx 560$, which, on the basis of past experience, is essentially equivalent to the limiting condition if x/R is not too large.

The results of most practical interest are, of course, related to the water produced per unit time per unit width of a single membrane for a given set of operating conditions. This quantity is given by

$$\begin{aligned} Q &= \int_0^x |v_w| dx \\ &= \frac{D}{3 N_{Sc}} \int_0^\sigma \frac{v_w}{(A \Delta P)} \left[\frac{\tau_w}{[\rho(A \Delta P^2)]} \right] \sigma^2 d\sigma \quad (24) \end{aligned}$$

or, in dimensionless form for wedge flows

$$Q^+ = \sigma^{2/(1-n)} \left[1 - 2 B_2 \sum_{k=0} \frac{\theta_k(0) \sigma^k}{k(1-n) + 2} \right]$$

where

$$\begin{aligned} Q^+ &= \frac{Q}{D} \left[\frac{(1-n) \phi''(0)}{6} N_{Sc}^{-[(1+3n)/2]} \right. \\ &\quad \times \left. \left(\frac{1+n}{2} \right)^{\frac{1}{2}} \left\{ \frac{(1-B_2) U_\infty}{v_w(0)} \right\}^{(3(n+1)/2)} \right. \\ &\quad \left. N_{Re_x}^{(-3n/2)} \right]^{-\{2/[3(1-n)]\}}. \end{aligned}$$

For fully developed flow between parallel plates

$$Q^+ = \sigma^3 - 3 B_2 \sum_{k=0}^{\infty} \theta_k(0) \frac{\sigma^{k+3}}{k+3}$$

where

$$Q^+ = \frac{3Q}{4D} N_{Re}(1 - B_2)^{-2} \left[\frac{v_w(0)}{U_b} \right]^2$$

Convenient quantities for discussing results are the fraction of total feed converted to pure water with a single membrane, Q_1 , which is given by

$$Q_1 = \frac{Q}{2 R U_b}$$

and the ratio of the fraction of feed converted to pure water to the fraction that would be converted if the transverse velocity at the wall remained equal to $v_w(0)$ along the entire conduit. We shall refer to the latter quantity as the efficiency, E , and it is given by

$$\begin{aligned} E &= \frac{Q}{v_w(0) x} \\ &= 1 - \frac{2 B_2}{1 - B_2} \sum_{k=1}^{\infty} \theta_k(0) \frac{\sigma^k}{2 + k(1-n)} \end{aligned}$$

DISCUSSION OF RESULTS

The preceding analysis is quite general in terms of flow conditions, and it enables one to make calculations rather easily for a number of systems once the appropriate functions have been determined. The functions which must be determined are, of course, the $\theta_k(\beta)$ for various

values of B_2 and n . In particular, to determine the build-up of salt along the conduit wall, and to calculate the productive capacity of a given system, the $\theta_k(0)$ must be known. $\theta_k(0)$ up to and including $\theta_9(0)$ are given in Table 1 for seven values of B_2 and $n = \frac{1}{3}$. Also, in Table 1 expansion coefficients are tabulated up to and including $\theta_5(0)$ in order to compare the behavior of the series for the case of $n = 0$ and $n = \frac{1}{3}$ with the case $v = 0$ for several values of B_2 . Furthermore, values of $\phi_{ij}(0)$ up to $i = j = 5$ are given in Table 2.

Figure 2 shows, for the various cases considered, how the wall concentration, and, therefore, the concentration polarization varies with

the boundary condition. This is to be expected since the finite velocity at the wall is due to the passage of water only, leaving salt to build up in concentration near the wall. On the other hand, convection toward the wall tends to reduce the salt concentration near the wall since material is brought in from less concentrated regions. Hence the predicted polarization is greater for the case of $v = 0$ than for $v = v_w$ in the diffusion equation. It is noted also that for a given σ the predicted polarization is greater for the case when the momentum and diffusion boundary layers begin at the same point, $n = 0$, than when the diffusion boundary layer begins in a fully developed velocity field, $n = \frac{1}{3}$. This is true be-

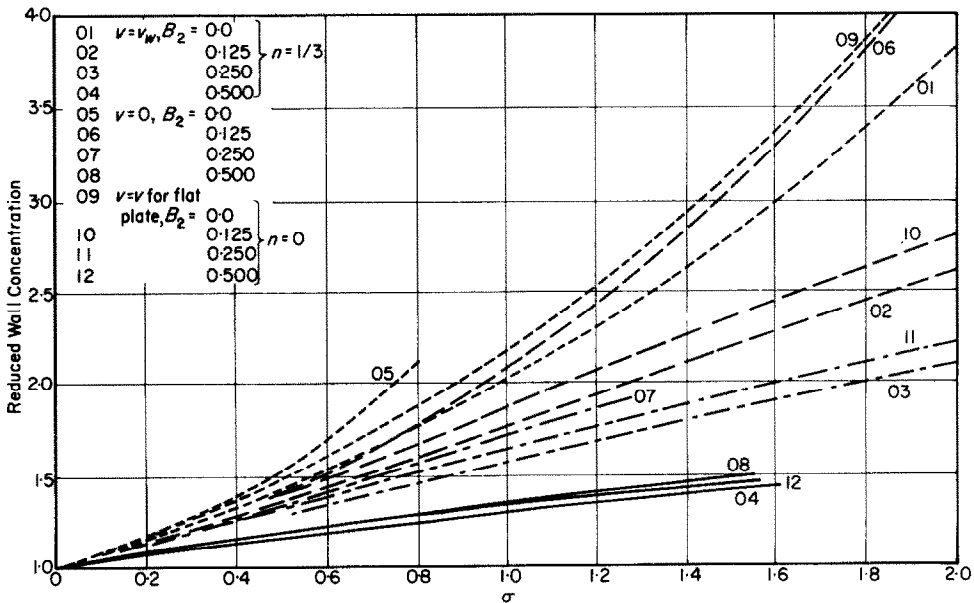


FIG. 2. Comparison of dimensionless wall concentration distributions in wedge flows for various values of B_2 and n . Solution for $n = \frac{1}{3}$ also correspond to fully developed flow between infinite parallel plates. Solutions for the case of $v = 0$, $n = \frac{1}{3}$ are included to illustrate error incurred by neglecting transverse velocity in differential diffusion equation.

σ for various B_2 . It should be remembered when viewing these data that the maximum possible value of $\theta_w(x, 0)$ is $1/B_2$. The effect of finite transverse velocity in the diffusion equation is seen to oppose the effect of finite transverse velocity in

cause of an additional convection effect away from the wall in the former case as the momentum boundary layer builds up. This effect is, of course, greatest very near the entrance. Although it cannot be seen clearly on Fig. 2, for

Table 1. Values of series coefficients $\theta_k(0)$
 $n = \frac{1}{3}$

B_2	$\theta_1(0)$	$\theta_2(0)$	$\theta_3(0) \times 10$	$\theta_4(0) \times 10^2$	$\theta_5(0) \times 10^3$	$\theta_6(0) \times 10^4$	$\theta_7(0) \times 10^5$	$\theta_8(0) \times 10^6$	$\theta_9(0) \times 10^7$
0	0.7385	0.2407	0.4384	0.4446	0.1591	0.1593	-0.1758	0.0466	0.1498
0.125	0.6462	0.1316	-0.0164	-0.8340	0.1309	5.435	6.251	-33.05	-80.42
0.15	0.6277	0.1125	-0.1734	-0.8186	0.6036	6.489	0.1695	-51.99	-42.34
0.25	0.5539	0.04509	-0.3261	-0.2926	3.075	2.033	-32.54	-13.29	363.7
0.334	0.4918	-0.00038	-0.3374	0.3683	3.227	-8.103	-30.04	138.7	228.6
0.5	0.3692	-0.06025	-0.1605	1.164	1.258	-13.24	59.47	29.22	-1061
0.75	0.1846	-0.07528	0.1950	0.0058	-3.217	18.37	-47.32	-73.72	1360

$n = 0$

B_2	$\theta_1(0)$	$\theta_2(0)$	$\theta_3(0) \times 10$	$\theta_4(0) \times 10^2$	$\theta_5(0) \times 10^3$
0.0	0.8219	0.3004	0.6214	0.7383	0.3655
0.125	0.7191	0.1673	-0.1177	-1.254	-0.5928
0.15	0.6986	0.1439	-0.2100	-1.255	0.5577
0.25	0.6164	0.06144	-0.4265	-0.5572	4.686
0.5	0.4109	-0.06828	-0.2357	1.608	-1.073

$v = 0$

B_2	$\theta_1(0)$	$\theta_2(0)$	$\theta_3(0)$	$\theta_4(0)$	$\theta_5(0)$
0.0	0.7385	0.4817	0.2868	0.1588	0.8289×10^{-1}
0.125	0.6462	0.3161	0.1101	0.1744×10^{-1}	0.8973×10^{-2}
0.15	0.6277	0.2866	0.8426×10^{-1}	0.2772×10^{-2}	-0.1370×10^{-1}
0.25	0.5539	0.1806	0.8116×10^{-2}	-0.2546×10^{-1}	-0.1207×10^{-1}
0.50	0.3692	0	-0.4058×10^{-1}	0	0.7820×10^{-2}

Table 2. Values of $\phi_{ij}(0)$, As defined by $\theta_i = (1 - B_2) \sum_{j=1}^i \phi_{ij} B_2^{j-1}$

$n = \frac{1}{3}$					
i/j	1	2	3	4	5
1	0.7385				
2	0.24074	-0.72247			
3	0.04384	-0.54666	0.78961		
4	0.00445	-0.21884	0.97054	-0.91500	
5	0.000159	-0.05707	0.61657	-1.5758	1.0990

very small σ the predicted polarization is greater for the former of the two cases just mentioned than for the case of $v = 0$ in the diffusion equation. For the class of flows considered here

$$-\frac{v}{A \Delta P} = 1 - B_2 \theta(\sigma, 0) + \frac{3n - 1}{3(1 - n)} \left[\frac{9}{2} \frac{\beta^2}{\sigma} \right] \quad (25)$$

and, therefore, when $n < \frac{1}{3}$ the last term contributes to increasing the value of v in the direction away from the membrane surface and thereby to increasing the concentration polarization for a given value of σ . It should be mentioned that this comparison is made only to show the effect of using different forms for v in the differential equation. The results will differ when translated from a given σ to x since the shear stress is different in the different systems.

The solution obtained for the case when the velocity profile is initially fully developed, i.e. $n = \frac{1}{3}$, should be quite accurate. It is likely, however that in practical systems the diffusion and momentum boundary layers will initiate at the same point. The solution obtained for the flat plate case, i.e. $n = 0$, will yield accurate results near the entrance of a conduit, but there is no clear means of extending the solution further downstream where the velocity profile becomes fully developed.

In the system being studied the diffusion boundary layer is very thin compared to the momentum boundary layer so that the velocity field is established much more rapidly than the concen-

tration field. Hence, it is reasonable to expect that the assumption of constant shear stress should apply over a relatively large fraction of the conduit length if it is long enough to obtain even a modest percentage of fresh water product from the saline feed solution. The problem is to find a suitable relationship for the term involving $d\tau_w/dx$ in equation (10). In the following discussion it will be shown that the extent of the hydrodynamic entrance region may be estimated by a method due to Sparrow [6], and that the shear stress in the entrance region may be approximated in terms of specific wedge type flows.

Following Sparrow,

$$\frac{u}{u_\delta} = 2 \frac{y}{\delta} - \left(\frac{y}{\delta} \right)^2$$

where δ is the boundary-layer thickness, u_δ is the velocity outside the boundary layer. Evaluating the shear stress from this form, we find

$$\tau_w = \frac{2\mu u_\delta}{\delta} \quad (26)$$

which yields the correct result, $\tau_w = (3 \mu U_b/R)$, for fully developed flow. It follows from equation (26) that

$$\int_0^x \frac{dx}{\tau_w(x)} = \int_0^x \frac{\delta dx}{2 \mu u_\delta}$$

Furthermore, Sparrow's analysis gives

$$\frac{\delta}{u_\delta} = \frac{3R}{u_\delta} \left(1 - \frac{U_b}{u_\delta} \right)$$

and

$$dx = \frac{3 R^2 U_b [(u_\delta/U_b) - 1] [9(u_\delta/U_b) - 7]}{10 (u_\delta/U_b)^2} \times d \frac{u_\delta}{U_b}$$

which yield

$$\int_0^x \frac{dx}{\tau_w(x)} = \frac{9 R^3}{20 \mu v} \left[9 \ln \frac{u_\delta}{U_b} + \frac{25}{u_\delta/U_b} - \frac{23}{(u_\delta/U_b)^2} + \frac{7}{(u_\delta/U_b)^3} - \frac{95}{6} \right]$$

Therefore we can derive a value for σ at the end of the hydrodynamic entrance region with no additional assumptions beyond Sparrow's, by setting $u_\delta/U_b = 1.5$ to get

$$\sigma_{f.d.} = 0.603 N_{Sc}^{\frac{1}{2}} \frac{N_{Re_w}}{1 - B_2}$$

When σ is larger than $\sigma_{f.d.}$ (which will be the case in most situations of practical interest since $(x/R)_{f.d.} = 0.026 N_{Re}$, and, as will be seen later, membrane lengths over 1000 radii may be required to produce even 1 or 2 per cent of the feed as fresh water) then it follows that

$$\sigma = \left\{ 0.22 N_{Sc}^2 \left(\frac{N_{Re_w}}{1 - B_2} \right)^3 + \frac{3}{16} \left(\frac{v_w(0)/U_b}{1 - B_2} \right)^3 \right. \\ \left. \times N_{Re} \left[\frac{x}{R} - \left(\frac{x}{R} \right)_{f.d.} \right] \right\}^{\frac{1}{2}} \\ = \frac{N_{Sc}^{\frac{1}{2}} N_{Re_w}}{1 - B_2} \left[-0.0917 + \frac{12}{N_{Re}} \frac{x}{R} \right]^{\frac{1}{2}}$$

It was possible to calculate $\sigma_{f.d.}$ easily, but it is much more difficult to employ Sparrow's results directly in the entrance region unless some additional, but reasonable, approximations are made. Thus it was found that the shear stress distribution in the inlet can be approximated fairly well by power functions as is the case of

wedge flows. In particular,

$$\tau_w = \begin{cases} \frac{0.96 \mu U_b}{R} x_1^{-0.382}, & 0.001 \leq x_1 \leq 0.01 \\ \frac{1.6 \mu U_b}{R} x_1^{-0.275}, & 0.01 \leq x_1 \leq 0.1 \end{cases} \quad (27)$$

where

$$x_1 = 16 \frac{x/4 R}{4 R U_b / v}$$

agrees with Sparrow's calculation within 10 per cent and $x_1 \simeq 0.1$ is the end of the hydrodynamic entrance region. Comparison of equation (27) with equation (14) shows that

$$n = \begin{cases} 0.079, & 0.001 \leq x_1 \leq 0.01 \\ 0.15, & 0.01 \leq x_1 \leq 0.1 \end{cases} \quad (28)$$

The important point demonstrated by equation (28) is that the correct inlet solution is between the cases $n = 0$ and $n = \frac{1}{3}$, and its continuation beyond the inlet region also will be between these curves shown on Fig. 2. Since the curves of n equals 0 and $\frac{1}{3}$, for a given B_2 , are reasonably close together for all values of B_2 , and cluster more closely for $B_2 \geq 0.25$, a crude but seemingly reasonable first approximation can be obtained by interpolation. Note also that the region of $n = 0.15$ comprises a much larger fraction of the conduit entrance length than does that related to $n = 0.079$. Thus a first approximation solution for the wall concentration distribution can be sketched on Fig. 2 by calculating $\sigma_{f.d.}$, locating the solution close to the midpoint between the n equals 0 and $\frac{1}{3}$ curves up to $\sigma_{f.d.}$ and then continuing the solution line parallel to the $n = \frac{1}{3}$ line.

Concentration distributions throughout an entire system can be determined if distributions for $\theta_k(\beta)$ are known. For $n = \frac{1}{3}$, such data, which involved $\theta_k(\beta)$ up to and including $\theta_5(\beta)$, are given in Figs. 3-6 for $B_2 = 0, 0.15, 0.25, 0.5$ and $n = \frac{1}{3}$.

It can be seen on Figs. 3-6 that the gradients of the $\theta_k(\beta)$ go essentially to zero at $\beta \simeq 1.5$.

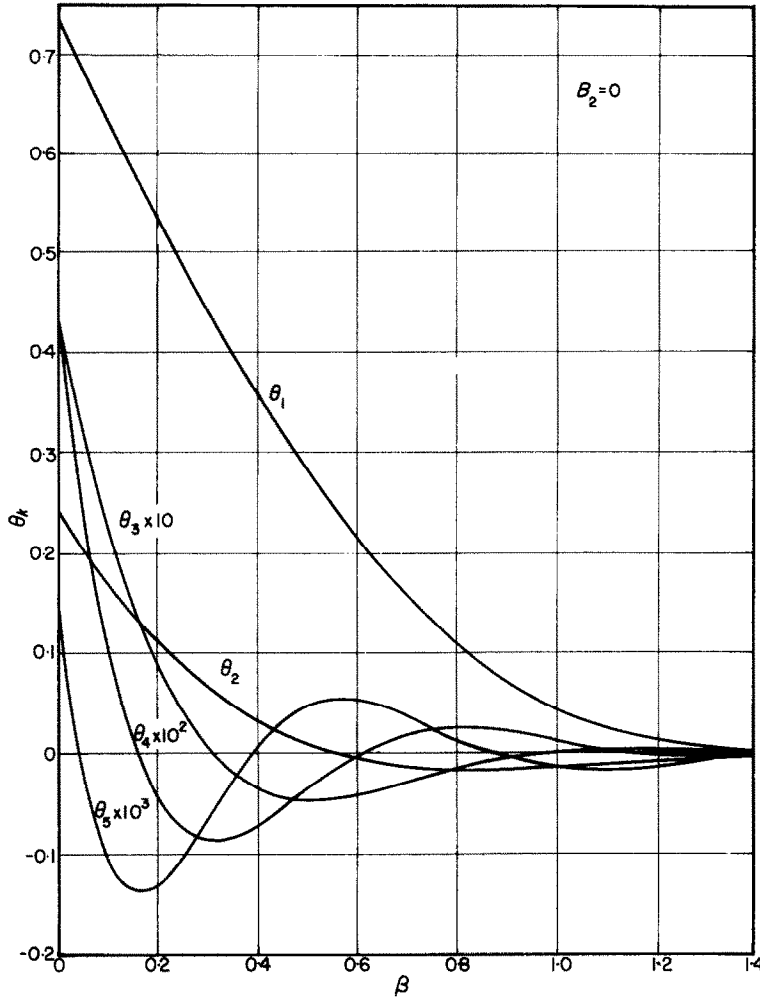


FIG. 3. Series expansion coefficients, $\theta_k(\beta)$, for case $B_2 = 0, n = \frac{1}{3}$.

Consequently, one can test the validity of linearizing the velocity to get equation (10) by estimating the diffusion boundary-layer thickness y_e . In the case of fully developed flow in parallel plate systems this thickness is given by

$$\frac{y_e}{R} = \left[\frac{12 x}{N_{Sc} N_{Re} R} \right]^{\frac{1}{3}} \beta_e \approx \left[\frac{12 x}{N_{Sc} N_{Re} R} \right]^{\frac{1}{3}} 1.5 \quad (29)$$

Except for very large values of x/R , it can be seen that y_e/R is small and the assumption is in fact a good one. Furthermore, equation (29)

can be used to estimate quantitatively the relative magnitudes of the two terms on the right-hand side of equation (9). For $B_2 = 0$, which as seen on Fig. 2 is when $d\tau_w/dx$ is most important, the ratio of the maximum value of the second term to the first term is about

$$\left(\frac{3}{2}\right)^3 \left[\frac{12 x}{N_{Sc} N_{Re} R} \right]^{\frac{1}{3}}$$

which is small unless x/R gets very large, but then equation (10) is invalid.

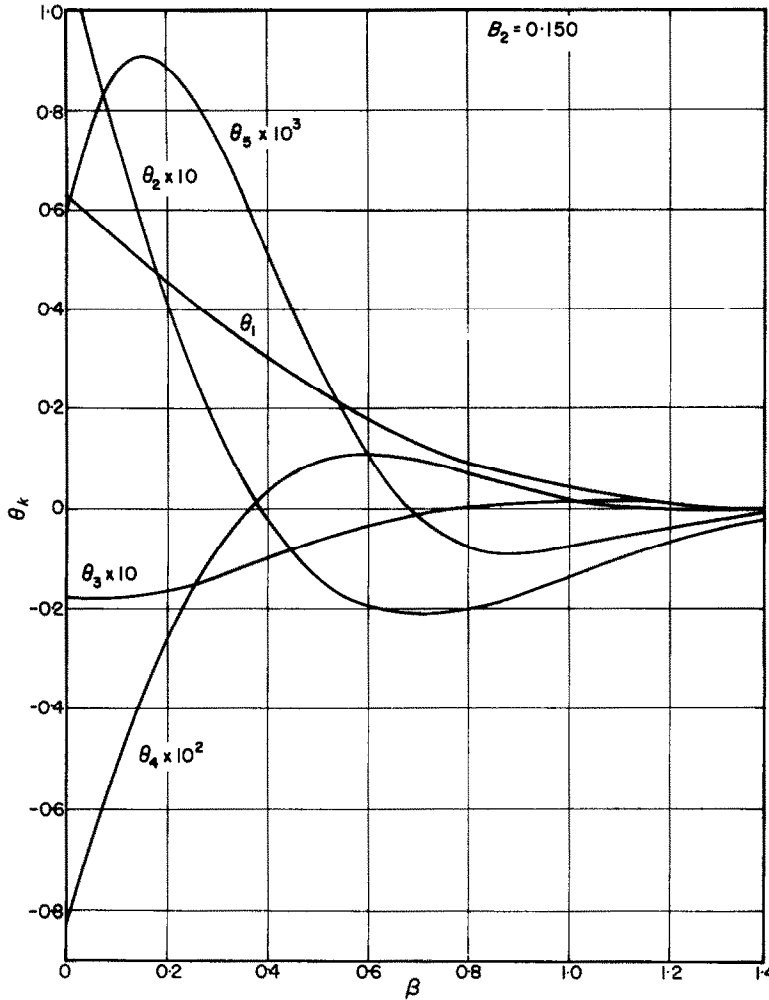


FIG. 4. Series expansion coefficients, $\theta_k(\beta)$, for case $B_2 = 0.15$, $n = \frac{1}{3}$.

The polarization was plotted versus σ for various B_2 in Fig. 2. Since the quantity B_2 is the ratio of the osmotic pressure at the channel inlet to the pressure drop across the membrane, one might at first thought expect the curves for various B_2 to represent the effects of varying the operating pressure. It is important to note, however, that B_2 appears in the definition of σ . If one wishes to analyse the effects of varying the operating pressure for a given membrane, as specified by the quantity A , and for a given osmotic pressure at the inlet, π_0 , then σ should

be written in the following form :

$$\begin{aligned} \sigma &= (9\lambda)^{\frac{1}{2}} \\ &= \left\{ 9 \frac{(A \Delta P)^3}{D^2} \mu \int_0^x \frac{dx}{\tau_w} \right\}^{\frac{1}{2}} \\ &= \left\{ 9 \left(\frac{A\pi_0}{B_2} \right)^3 \frac{\mu}{D^2} \int_0^x \frac{dx}{\tau_w} \right\}^{\frac{1}{2}} \end{aligned}$$

Hence, to obtain a coordinate which is dependent upon the axial distance and fixed parameters,

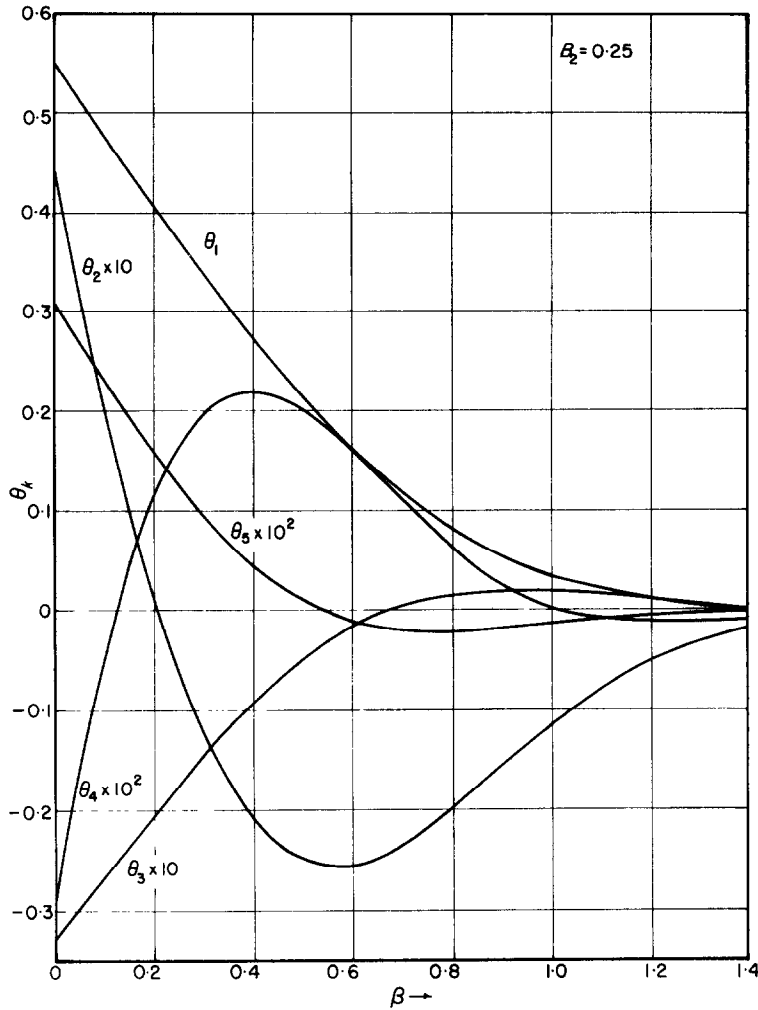


FIG. 5. Series expansion coefficients, $\theta_k(\beta)$, for case $B_2 = 0.25, n = \frac{1}{3}$.

one should use the quantity σB_2 or $(\sigma B_2)^3$. Similarly, B_2 is implicit in the definition of the dimensionless water production parameter, Q^+ . Hence, when considering the effects of varying the operating pressure on water production one should use the parameter $Q^+ B_2^{(1+n)/(1-n)}$.

In the light of the preceding discussion the effects of varying the operating pressure for the case $n = \frac{1}{3}$ were analysed by plotting $Q^+ B_2^2$ and E vs. $(\sigma B_2)^3$, as shown in Figs. 7(a) and 7(b), respectively. It is apparent that as one increases the operating pressure (i.e.

decreases B_2) the water production increases, but that E , the ratio of the water produced to that which would be produced if no polarization occurred, decreases. Hence the total production increases, but the efficiency of the system decreases as the operating pressure increases.

A simple relationship exists between $Q^+ B_2^2$ and E , as given by

$$Q^* = Q^+ B_2^2 = \frac{1 - B_2}{B_2} (\sigma B_2)^3 E.$$

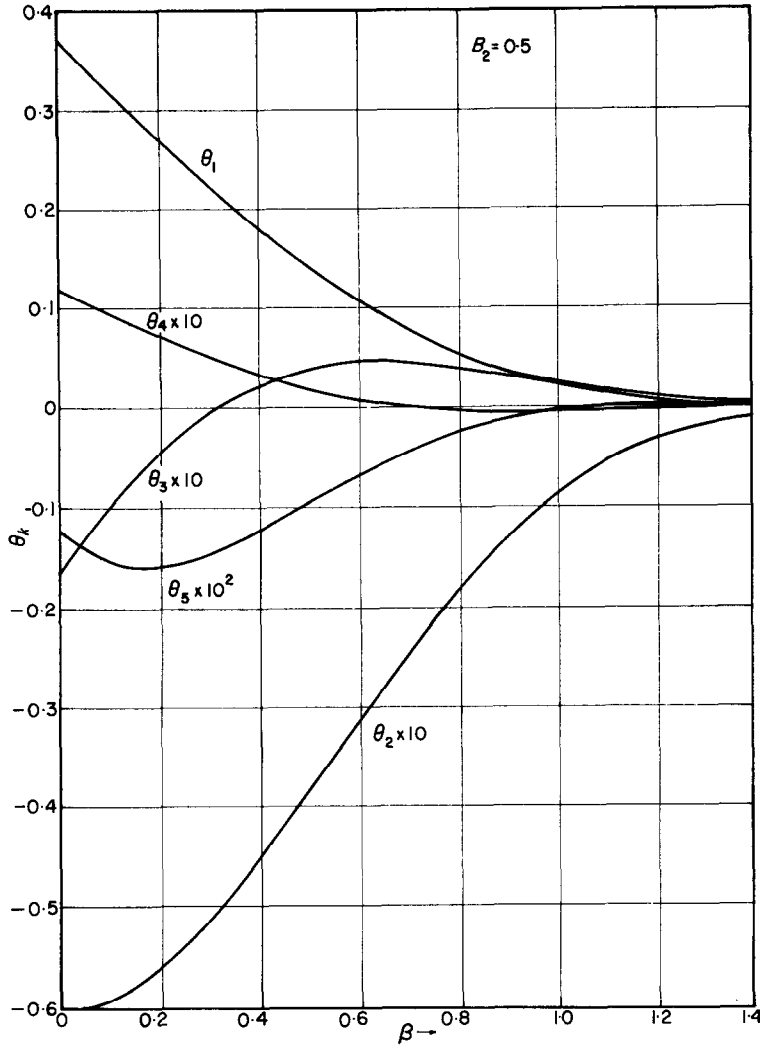


FIG. 6. Series expansion coefficients, $\theta_k(\beta)$, for case $B_2 = 0.5$, $n = \frac{1}{3}$.

It is noteworthy that the length of membrane required to produce a given amount of water decreases very rapidly as the operating pressure increases.

Figures 8 and 9 give a reasonable idea of how typical parallel plate systems behave in terms of parameters which can be visualized more easily. Figure 8 indicates how the salt concentration at the wall builds up more rapidly as the membrane capacity increases. In contrast, Fig. 9 shows that a much larger fraction of the feed is produced as the membrane capacity increases.

The polarization is seen to be significantly decreased by increasing the bulk velocity. However, as the bulk velocity increases the fraction of the feed produced as pure water for a given membrane length decreases. Hence in determining the optimal system design one must balance the two factors. A greater total quantity of water is produced for a higher bulk velocity, but this is achieved at the cost of greater pumping requirements.

Figure 10 compares our series solution for $n = \frac{1}{3}$ with Dresner's solution, which applies to

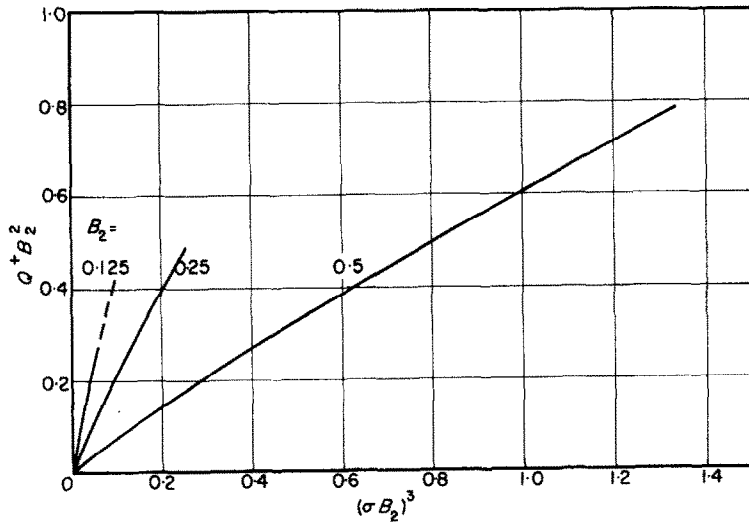


FIG. 7(a). Variation of system productivity for several values of B_2 as a function of dimensionless system length.

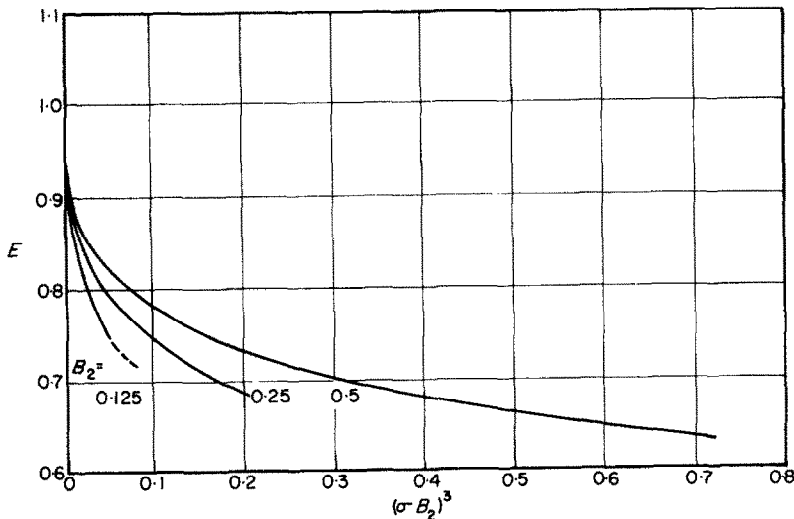


FIG. 7(b). Variation of system efficiency, E , for several values of B_2 as a function of dimensionless system length.

fully developed flow in a flat plate conduit with constant v_w , and is given by

$$\theta_D = 1 + \epsilon + 5 \{1 - \exp[-\sqrt{(\epsilon/3)}]\} \quad (31)$$

where

$$\epsilon = \frac{[(1 - B_2) \sigma]^3}{9}$$

In order to make such a comparison the v_w in equation (31) was taken to be $v_w(0)$. Naturally, this tends to exaggerate the concentration build-up at large σ . However, no really satisfactory method for estimating an average, v_w , other than using our series expansion results, can be specified *a priori*.

The reverse osmosis problem posed here and

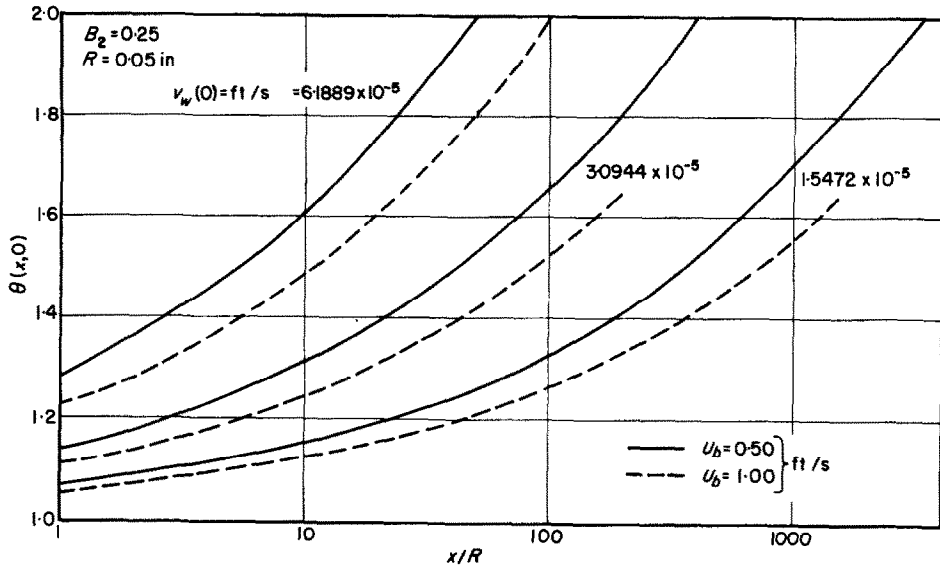


FIG. 8. Effect of membrane capacity, $v_w(0) = A \Delta P[1 - B_2]$, and system velocity, U_b , on salt concentration at the membrane surface as a function of channel length.

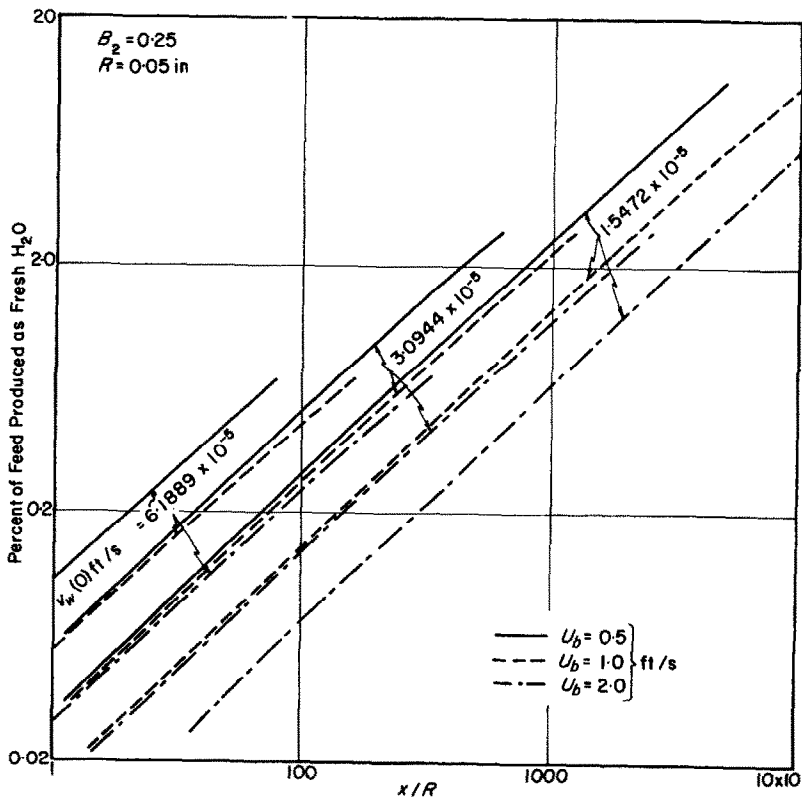


FIG. 9. Effect of membrane capacity, $v_w(0) = A \Delta P[1 - B_2]$, and system velocity, U_b , on the percentage of feed produced as fresh water as a function of system length.

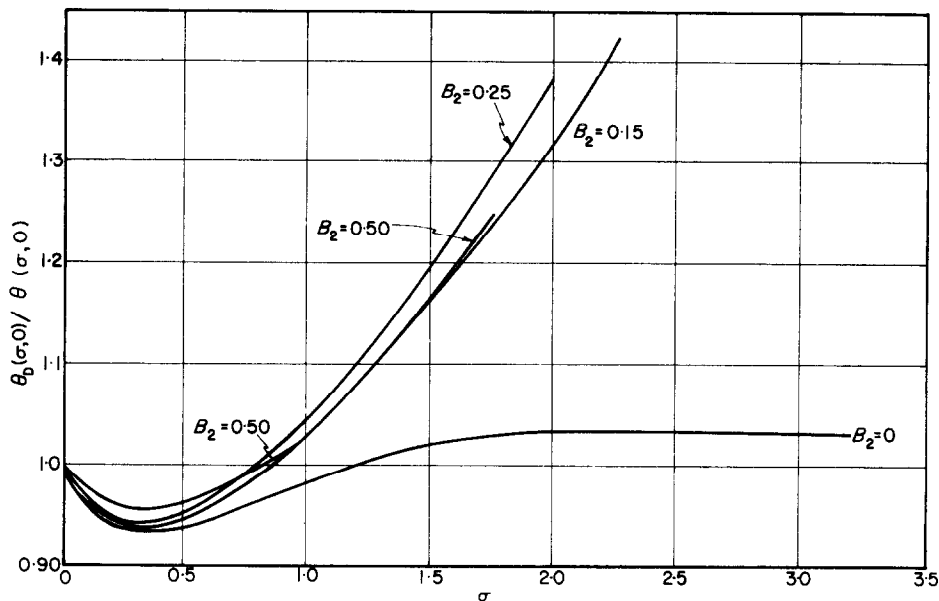


FIG. 10. Ratio of Dresner's solution, equation (31), to series expansion solution.

and the one solved by Dresner become identical mathematically only when $B_2 = 0$. In this case, it is seen that for $\sigma \geq 2.0$ the ratio $\theta_D(\sigma, 0)/\theta(\sigma, 0)$ is essentially constant at 1.04. In the region $\sigma \leq 1$, where the series expansion is more accurate, it is seen that $\theta_D(\sigma, 0)$ underestimates the concentration build-up slightly, the ratio always being equal to or greater than about 0.93.

Dresner recognized the inaccuracy of equation (31) very near the inlet, and proposed an alternate form for that region:

$$\theta(\epsilon, 0) = 1 + 1.536 \epsilon^{\frac{1}{3}}$$

or

$$= 1 + \frac{1.536}{\sqrt[3]{9}} (1 - B_2) \sigma. \quad (32)$$

As may be seen from equation (22), this solution corresponds to the first two terms of the present series solution, $\theta(\sigma, 0) = 1 + \theta_1(0) \sigma$. Inspection of the values of $\theta_2(0)$ for various B_2 indicates that equation (32) will be accurate within about 10 per cent for $\sigma < 0.5$ for the range of B_2 considered.

COMPARISON OF THEORY WITH EXPERIMENTAL DATA

Very few data are available in the literature which can be used to test the theory developed previously. No detailed experimental studies of local diffusional effects in reverse osmosis systems were found. However, it will be shown that the results of the work of Merten, Lonsdale and Riley [3], who, for $B_2 = 0.334$, studied the overall effects of concentration polarization on the productive capacity of reverse osmosis systems, do agree reasonably well with the present theory.

Merten *et al.* studied reverse osmosis in two cells with different membranes, designated 1 and 2, for which the membrane constants determined by their method are 7.6 and 6.8×10^{-6} g/cm² s atm. In determining the membrane constant they made runs at 200 cm/s and at this velocity they assumed that the polarization was negligible. This is not exact and thus these membrane constants are somewhat low.

Five experiments in the laminar range with membrane 1 were made at velocities ranging approximately from 6 to 48 cm/s. Differences

between present theory and these experimental results range to a maximum of about 10 per cent, and the overall agreement would be improved substantially if the membrane constant is increased by 5 or 10 per cent. In the region of these experiments the cell productive capacity is quite insensitive to changes in flow rate and therefore the agreement between theory and experiment is merely suggestive and certainly not conclusive.

In contrast to the experiments with membrane 1, the data obtained with membrane 2 were taken in a region where the average cell productivity varies more rapidly with the bulk mean brine velocity in the channel which approximately ranged from 0.2 to 2.0 cm/s. Perhaps it is most significant that Merten, Lonsdale and Riley proposed a theory to explain their data and it is in this range of conditions for membrane experiments where significant differences exist between the present

work and the correlation of reference [3]. In particular, with $A = 6.8 \times 10^{-5}$ g/cm² s atm, the average percentage error between calculated and observed values is estimated to be about 35 per cent for their correlation and about 5 per cent for the present theory.

REFERENCES

1. L. DRESNER, Boundary layer build-up in the demineralization of salt water by reverse osmosis, ORNL-3621 (May 1964).
2. W. N. GILL, C. TIEN and D. W. ZEH, Concentration polarization effects in a reverse osmosis system, *I/EC Fundamentals* 4, 433 (1965).
3. U. MERTEN, H. K. LONSDALE and R. L. RILEY, *I/EC Fundamentals* 3, 210 (1964).
4. T. K. SHERWOOD, P. L. T. BRIAN, R. E. FISHER and L. DRESNER, Salt concentration at phase boundaries in desalination processes, *I/EC Fundamentals* 4, 113 (1965).
5. A. S. BERMAN, *J. Appl. Phys.* 24, 1232 (1953).
6. E. M. SPARROW, NACA TN 3331 (1955).
7. H. SCHLICHTING, *Boundary Layer Theory*, 4th edn. McGraw-Hill, New York (1960).

Résumé—On expose la théorie des écoulements bidimensionnels avec osmose à contre-courant et à pression constante de telle façon que les performances soient prévues d'une façon explicite en fonction des variables en jeu. De tels problèmes nécessitent la solution d'une équation non linéaire de la diffusion avec des conditions aux limites nonlinéaires. Une solution en série est obtenue qui tient compte des nonlinéarités à la fois dans l'équation de la diffusion et dans ses conditions aux limites.

Les couches limites avec gradient de pression sont considérées comme des écoulements sur des drièdres et la théorie peut être appliquée à la fois pour l'écoulement entièrement établi et dans la région d'entrée. Les résultats numériques généralisés sont donnés dans une large gamme ayant un intérêt pratique. Quelques résultats spécifiques sont également exposés pour des systèmes typiques semblables à ceux qui peuvent être employés en pratique.

Zusammenfassung—Analysen von kontinuierlichen zweidimensionalen Strömungssystemen der umgekehrten Osmose bei konstantem Druck sind so wiedergegeben, dass die Systemleistung explizit in Abhängigkeit von den Betriebsveränderlichen ermittelt werden kann. Derartige Probleme erfordern die Lösung einer nichtlinearen Diffusionsgleichung mit nichtlinearen Randbedingungen. Eine Reihenlösung, die Nichtlinearitäten sowohl in der Diffusionsgleichung berücksichtigt als auch in ihren Grenzbedingungen, wurde entwickelt.

Grenzschichtströmungen mit Druckgradienten werden als Keilströmungen behandelt und die angegebenen Analysen können auf die voll ausgebildete und die Einlaufströmung angewandt werden. Verallgemeinerte numerische Ergebnisse werden für einen weiten Bereich des praktischen Interesses gefunden. Einige spezifische Daten werden angegeben für typische Systeme ähnlich den in der Praxis verwendeten.

Аннотация—Проведен анализ непрерывных систем с двумерными обратноосмотическими потоками при постоянном давлении. Характеристика таких систем рассчитывается в явном виде с помощью рабочих параметров. Такие задачи требуют решения нелинейного уравнения диффузии при нелинейных граничных условиях. Получен ряд решений с учетом нелинейности уравнения диффузии и граничных условий.

Течения в пограничном слое с градиентом давления аналогичны оттеканию клина. Приведенный анализ можно применить как к полностью развитому течению, так и входному участку. Представлены обобщенные численные результаты для широкого диапазона исследованных параметров. Приведены также некоторые данные для систем, представляющих практический интерес.